Radiation Protection Dosimetry (year), Vol. 0, No. 0, pp. 0–0
DOI: 10.1093/rpd/nc0000

MEASUREMENTS OF THE NEUTRON ACTIVATION CROSS SECTIONS FOR BI AND CO AT 386 MEV

H. Yashima[1*], S. Sekimoto[1], K. Ninomiya[2], Y. Kasamatsu[2], T. Shima[3], N. Takahashi[2], A. Shinohara[2], H. Matsumura[4], D. Satoh[5], Y. Iwamoto[5], M. Hagiwara[4], K. Nishiizumi[6] M. W. Caffee[7], and S. Shibata[1]
[1]Research Reactor Institute, Kyoto University, Kumatori, Osaka, 590-0494, Japan
[2]Graduate School of Science, Osaka University, Toyonaka, Osaka, 560-0043, Japan
[3]Research Center for Nuclear Physics, Osaka University, Suita, Osaka, 567-0047, Japan
[4]High Energy Accelerator Research Organization, Tsukuba, Ibaraki, 305-0801, Japan
[5]Japan Atomic Energy Agency, Tokai-mura, Naka-gun, Ibaraki, 319-1195, Japan
[6]Space Sciences Laboratory, University of California, Berkeley, CA 94720-7450, USA
[7]Department of Physics, Purdue University, West Lafayette, IN 47907, USA

Received month date year, amended month date year, accepted month date year

Neutron activation cross sections for Bi and Co at 386 MeV were measured by activation. Quasi-monoenergetic neutron were produced using the ^{7}Li(p,n) reaction. The energy spectrum of these neutrons has a high-energy peak (386 MeV) and a low-energy tail. Two neutron beams, 0° and 25° from the proton beam axis, were used for sample irradiation, enabling a correction for the contribution of the low-energy neutrons. The neutron activation cross sections were estimated by subtracting the reaction rates of irradiated samples for 25° degree irradiation from those of 0° irradiation. The measured cross sections were compared with the findings of other studies, evaluated in relation to nuclear data files and the calculated data by PHITS code.

INTRODUCTION

Countless experiments undertaken in the last 50 years at nuclear facilities provide nuclear database that serves as an archive of information used routinely by scientists and engineers. Among these data are activation cross sections for high-energy neutrons; data needed for estimation of residual radioactivities in accelerator facilities, delineating cosmic-ray irradiation histories of extraterrestrial matter, and neutron dosimetry of high energy neutron fields. While there are numerous measurements of activation cross sections for neutrons having energy below 20 MeV, comparable measurements for energies above 20 MeV are scarce(1-5); there are no measurements above 200 MeV. In lieu of measurements, neutron-activation cross sections are evaluated on the assumption that neutron-induced cross sections above 100 MeV are approximately equal to proton-induced cross sections of the same energy or by theoretical model calculation. The cross section data of ^{209}Bi(n, xn) and ^{59}Co(n, xn) reactions, in particular, were reported for energies up to 150 MeV(1,2), and these have been applied to high energy neutron spectrometry(6-8). But calculation of the neutron-induced activation above 150 MeV is problematic due to absence of experimental data.

We have undertaken a systematic measurement of activation cross sections for high-energy neutrons(9-12). In this measurement, a neutron beam is produced via the ^{7}Li(p,n) reaction. While this reaction produces a quasi-monoenergetic neutron beam it does have a small low-energy tail. Our methodology makes a correction for this low-energy tail and is based on measuring these activation cross sections using two different irradiation geometries, one is which the target is placed at a location 0° offset from the axis of the proton beam and the other is offset at 25° for proton beam axis to correct for low-energy neutron production(5). We report in this work the neutron activation cross sections of Bi and Co for 386 MeV neutrons. Bi and Co were chosen because of their application to high energy neutron spectrometry as described above and following reason: (a) ^{209}Bi and ^{59}Co are 100% abundance of each element so that easy to study nuclear systematic. (b) Bi is a good target for both spallation and fragmentation reactions. (c) Co is a good target for middle mass (near Fe). The measured experimental results are compared with other experimental data (neutron-induced and proton-induced), calculated data using the Particle and Heavy Ion Transport code System(13,14) (PHITS), and archived evaluated nuclear data.

EXPERIMENT

Protons for the ^{7}Li(p,n) reaction were provided by a ring-cyclotron at the Research Center for Nuclear Physics (RCNP), Osaka University. The quasi-monoenergetic neutrons were emitted from a 1-cm-thick ^{nat}Li target, bombarded with 389 MeV protons. The neutrons emitted in the forward direction traveled into the time-of-flight (TOF) room through an iron collimator (12×10 cm^{2} aperture) that was embedded

*Corresponding author: yashima@rri.kyoto-u.ac.jp

© The author (year). Published by Oxford University Press; all rights reserved

inside a 150-cm-thick concrete wall. Charged particles such as secondary proton produced from Li target and accelerator component are deflected and stopped in the collimator with the aid of a bending magnet placed within the collimator.

The neutron spectra were measured using TOF. A NE213 liquid scintillation detector was placed at the 0˚ position, then later at the 25˚ directions. A schematic view of the experimental set up is shown in Fig. 1.

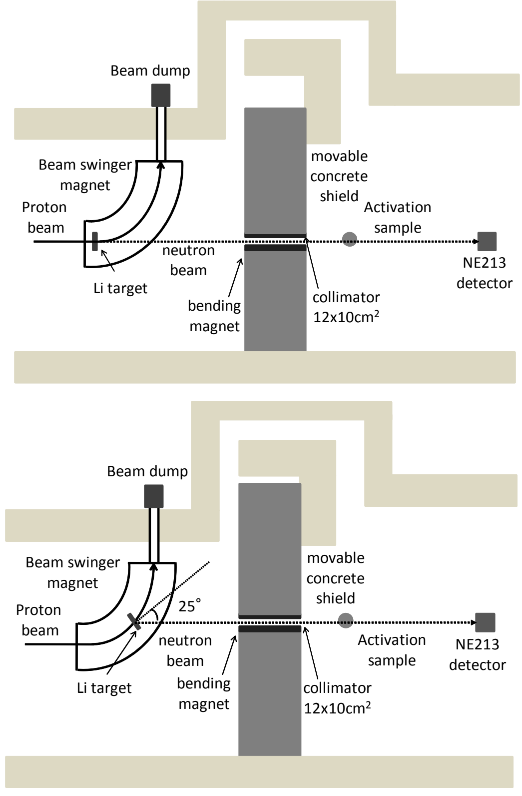

Figure 1. Schematic view of the experimental set up. (upper panel:0˚ irradiation, lower panel:25˚ irradiation)

The neutron flight time was measured as the temporal difference between the timing signal from the accelerator and the neutron detector signal. The neutron spectra were obtained after corrections for detector solid angle, proton beam current and detection efficiency (calculated using SCINFUL-QMD[15,16]). The measured neutron spectra are shown in Fig. 2. Two types of irradiation were performed in this study. The Bi (3cm x 3cm x 2mm) and Co (3cm x 3cm x 1mm) samples were placed at an angle of 0˚ to the proton beam to measure activities induced by the quasi-monoenergetic high-energy neutrons, comprising the peak, and the low energy neutrons, comprising a low-energy tail. Bi and Co placed at the 25˚ offset position undergo reactions induced by only the low energy neutrons, that is those that form a tail that closely mimics the tail of the 0˚ line[17]. The distances between the Li target and the samples for the 0˚ and 25˚ positions were 8.05 m and 7.19 m, respectively. The durations of the irradiations for the 0˚ and 25˚ positions were 31.6 hours and 23.3 hours, respectively. The average proton beam intensity was ~1 μA. The proton current at the beam dump was recorded with a digital current integrator, connected to a multi-channel scaler (MCS) to monitor the fluctuations of the proton beam. After irradiation, gamma rays emitted from the samples were measured with a high-purity germanium (HPGe) detector. The samples were measured repeatedly to aid identification of radioactive species by their half-lives.

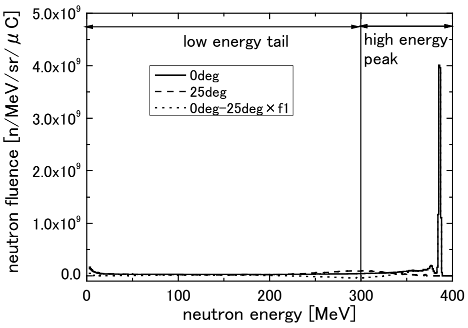

Figure 2. Neutron energy spectra generated by the ^{7}Li(p,n) reaction and corrected spectra obtained by subtracting the normalized 25˚ spectra from the 0˚ spectra.

DATA ANALYSIS

The physical properties of the radioactive nuclides measured in this study are listed in Table 1[18].

The reaction rates of the radioactive nuclides produced in the samples were determined from the gamma-ray spectra and the decay curves. Corrections to the data were made for beam current fluctuations using the digitized proton current and the peak efficiency of the HPGe detector using the EGS4 code[19].

The measured neutron spectrum at the 0˚ position shows a high-energy peak and a low-energy tail (Fig. 2); the high-energy peak prominent at 0˚ is absent from the 25˚ position. The energies of the peak neutrons are in the range 300-400 MeV; the energy ranges of the low-energy neutron are 3-300 MeV. The mean neutron energy for the high-energy peak is 386 MeV; the uncertainties in this peak energy of the corrected spectrum evaluated from the FWHM of high-energy peak, is 1 MeV. To correct for the nuclides produced by the low-energy neutrons, the 25˚ spectrum is first normalized (using neutron fluence of low-energy tail) to the one measured at 0˚, and then subtracting the activity produced by the normalized 25˚ spectrum (Fig. 2) from the one produced by the 0˚ spectrum, leaving only the activity produced by neutrons comprising the high-energy peak. The cross section for the peak neutron energy, σ, is given by:

$$\sigma = \frac{R_0 - R_{25} f_1 f_2}{\phi_{peak}} \qquad (1)$$

where R_0 and R_{25} are the reaction rates(1/atom/μC) for 0° and 25° irradiation, respectively, f_1 is the normalization factor to equalize the neutron fluence in the low energy range, 0.84, f_2 is the correction factor for the distances between the Li target and the samples, 0.80 and Φ_{peak} is the high-energy peak neutron fluence of corrected spectra, 2.16×10^4 n/cm^2/μC. Contributing to the estimation of uncertainty in the cross section measurements are the counting statistics (<30%), detector efficiency (Ge detector (10%), NE213 detector (15%)), beam current monitoring (5%) and correction for contribution of low energy tail (10%).

RESULTS AND DISCUSSION

The cross sections obtained for ^{209}Bi(n,xn) $^{201, 202, 203, 204, 205, 206}$Bi, ^{209}Bi(n,x)^{183g}Os, ^{209}Bi(n,x)$^{200, 201}$Pb, ^{59}Co(n,xn)^{56,57,58}Co, ^{59}Co(n,x)^{52,54}Mn reactions are tabulated in Table 2. The cross sections obtained for ^{209}Bi(n,xn) $^{201, 206}$Bi, ^{209}Bi(n,x)^{183g}Os, ^{209}Bi(n,x)^{200}Pb, ^{59}Co(n,xn)^{56,57,58}Co, ^{59}Co(n,x)^{54}Mn reactions are shown in Figs. 3(a)-(d) and Figs. 4(a)-(d), respectively. The shaded square symbols are the results of this work, the open square symbols are our previous results(11), and the other open symbols are literature data from Kim et al.(1,2), Michel et al.(20) and Schiekel et al.(21). We compare our results to the proton-induced reaction determined by Michel et al.(20) and Schiekel et al.(21) since there are few neutron activation data above 200 MeV. The curves shown in Figs. 3 and 4 are derived from Japanese Evaluated Nuclear Data Library High Energy File(22,23) (JENDL-HE). In JENDL-HE data, there is a gap around 250 MeV, because two different calculation models were used for JENDL-HE evaluation(22,23). The open inverted triangle symbols are results from PHITS(ver.2.52) calculations(13,14).

For those excitation functions shown in Figs.3(a-d), ^{209}Bi, we conclude: (1) the latest measurement agrees with our previous results(11) and those of Michel(20); (2) JENDL-HE(22,23) cross sections are generally lower than our measurements, ^{183g}Os are the exceptions; and (3) PHITS calculations produce cross sections lower than our measurements.

For those excitation functions shown in Figs.4(a-d), ^{59}Co, we conclude: (1) the latest measurement agrees with those of Schiekel(21) except for ^{56}Co, in Figs.4 (a-c), the difference between p-induced and n-induced cross sections of ^{59}Co(n,xn) reaction is smaller for smaller x; and (2) cross sections based on JENDL-HE(22,23)data and PHITS calculations(13,14) agree with our measurements, except for ^{54}Mn. The JENDL-HE data and PHITS calculations do not always agree with our measurements, providing further impetus for more direct measurements of neutron-induced activation cross sections.

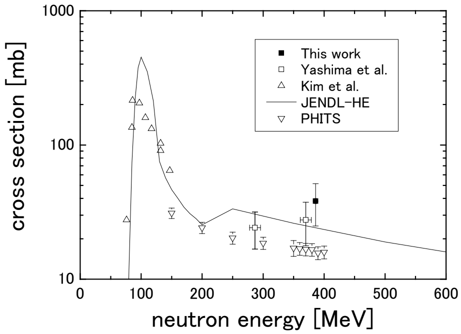

Figure 3(a). Excitation function for ^{209}Bi(n,9n) ^{201}Bi reaction

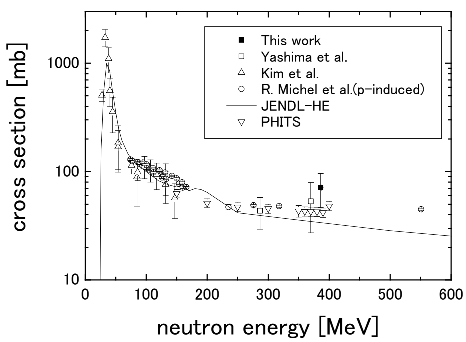

Figure 3(b). Excitation function for ^{209}Bi(n,4n) ^{206}Bi reaction

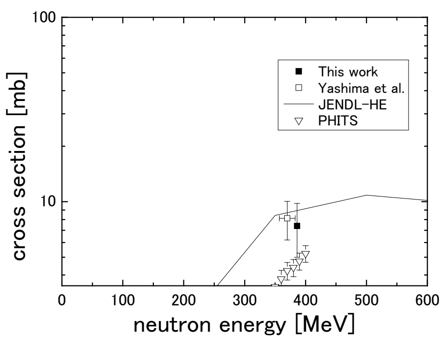

Figure 3(c). Excitation function for ^{209}Bi(n,x) ^{183g}Os reaction

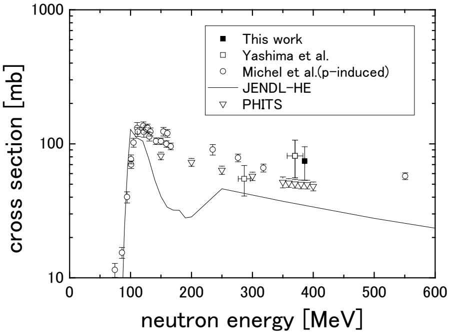

Figure 3(d). Excitation function for $^{209}Bi(n,x)\ ^{200}Pb$ reaction

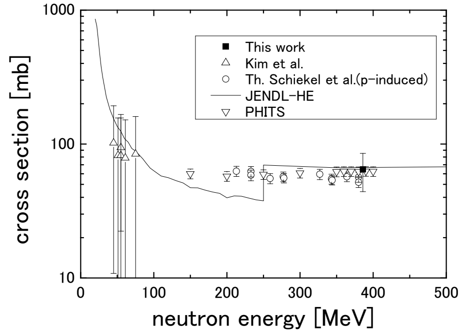

Figure 4(c). Excitation function for $^{59}Co(n,2n)^{58}Co$ reaction

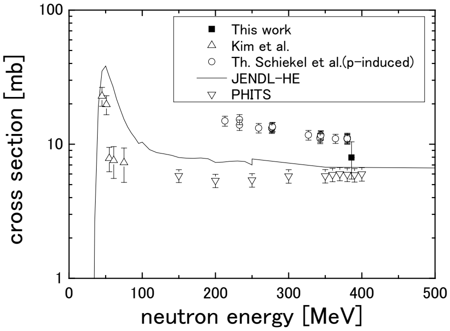

Figure 4(a). Excitation function for $^{59}Co(n,4n)^{56}Co$ reaction

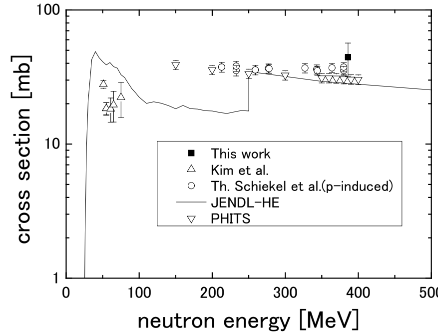

Figure 4(d). Excitation function for $^{59}Co(n,x)^{54}Mn$ reaction

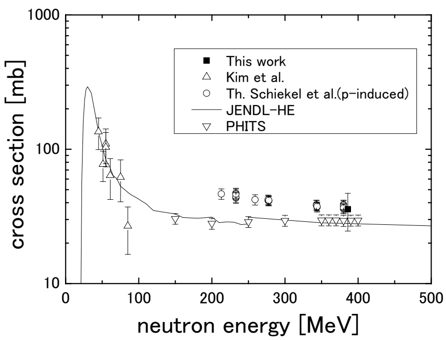

Figure 4(b). Excitation function for $^{59}Co(n,3n)^{57}Co$ reaction

SUMMARY

The cross sections for the production of short-lived radionulides from neutron activation of Bi and Co at 386 MeV were directly measured by nuclear decay counting methods. A quasi-monoenergetic neutron beam was produced using the $^{7}Li(p,n)$ reaction. These experimental results are useful both as benchmark data for evaluating nuclear data and for validating the accuracy of codes used to calculate neutron cross sections.

ACKNOWLEDGMENTS

The authors express their gratitude to the accelerator staff of RCNP for generous support during this experiment.(RCNP-E298) This study was supported by the Ministry of Education, Science, Sports and Culture by a Grant-in-Aid for Young Scientists (B) (no. 25870367). This work was also supported by NSF and NASA grants.

REFERENCES

1. Kim, E., Nakamura, T., Konno, A., Uwamino, Y., Nakanishi, N., Imamura, M., Nakao, N., Shibata, S. and Tanaka, S. Measurements of neutron spallation cross sections of ^{12}C and ^{209}Bi in the 20- to 150-MeV energy range. Nucl. Sci. and Eng., **129**, 209-223 (1998).
2. Kim, E., Nakamura, T., Uwamino, Y., Nakanishi, N., Imamura, M., Nakao, N., Shibata, S. and Tanaka, S. Measurements of activation cross sections on spallation reactions for ^{59}Co and ^{nat}Cu at incident neutron energies of 40 to 120 MeV. J. Nucl. Sci and Technol., **36**, No.1, 29-40 (1999).
3. Glasser, W., Michel, R., Neumann, S., Schuhmacher, H., Dangendorf, V., Nolte, R., Herpers, U., Smirnov, N. A., Ryzhov, I., Prokofiev, V. A., Malmborg, P., Kollar, D. and Meulders, P. J. Radionuclide production from lead by neutron-induced reactions up to 175 MeV. J. Nucl. Sci and Technol., supplement **2**, 373 (2002).
4. Yashima, H., Terunuma, K., Nakamura, T., Hagiwara, M., Kawata, N. and Baba, M. Measurement of neutron activation cross sections for major elements of water, air and soil between 30 and 70 MeV. J. Nucl. Sci and Technol., supplement **4**, 70-73 (2004).
5. Sisterson, J. M., Brooks, F. D., Buffler, A., Allie, M. S., Jones, D. T. L. and Chadwick, M. B. Cross-section measurements for neutron-induced reactions in copper at neutron energies of 70.7 and 110.8 MeV. Nucl. Instr. and Meth., B**240**, 617 -624(2005).
6. Kasugai, Y., Takada, H. and Ikeda, Y. Dosimetry of a GeV proton-driven spallation neutron field by the activation method. Reactor Sosimetry: Radiation Metrology and Assessment, ASTM STP 1398, John G. Williams, David W. Vehar, Frank H. Ruddy, and David M. Gilliam, Eds., American Society for Testing and Materials, West Conshohocken, PA(2001)
7. Maekawa, F., Meigo, S., Kasugai, Y., Takada, H., Ino, T., Sato, S., Jerde, E., Glasgow, D., Niita, K., Nakashima, H., Oyama, Y., Ikeda, Y., Watanabe, N., Hastings, J. and The ASTE Collaboration Analysis of a neutronic experiment on a simulated Mercury spallation neutron target assembly bombarded by giga-electron-volt protons. Nucl. Sci. and Eng., **150**, 99-108 (2005).
8. Yashima, H., Kasugai, Y., Matsuda, N., Matsumura, H., Sekimoto, S., Toyoda, A., Iwase, H., Mokhov, N., Leveling, A., Boehnlein, D., Vaziri, K., Oishi, K., Nakashima, H. and Sakamoto, Y. Spatial distribution measurement of neutrons produced by 120-GeV proton beam in concrete shield. Prog. Nucl. Sci and Technol., **3**, 40-43 (2012).
9. Nishiizumi, K., Welten, K. C., Matsumura, H., Caffee, M. W., Ninomiya, K., Omoto, T., Nakagaki, R., Shima, T., Takahashi, N., Sekimoto, S., Yashima, H., Shibata, S., Bajo, K., Nagao, K., Kinoshita, N., Imamura, M., Sisterson J. and Shinohara, A. Measurements of high-energy neutron cross sections for accurate cosmogenic nuclide production rates, Geochim. Cosmochim. Acta 73, A945(2009).
10. S. Sekimoto, S., Utsunomiya, T., Yashima, H., Ninomiya, K., Omoto, T., Nakagaki, R., Shima, T., Takahashi, N., Shinohara, A., Kinoshita, N., Matsumura, H., Satoh, D., Iwamoto, Y., Hagiwara, M., Nishiizumi, K. and Shibata, S., Measurement of Neutron Cross Sections for Yttrium and Terbium at 287 MeV, Prog. Nucl. Sci. Technol. 1, 89-93(2011).
11. Yashima, H., Sekimoto, S., Utsunomiya, T., Ninomiya, K., Omoto, T., Nakagaki, R., Shima, T., Takahashi, N., Shinohara, A., Matsumura, H., Satoh, D., Iwamoto, Y., Hagiwara, M., Nishiizumi, K. and Shibata, S., Measurements of the neutron activation cross sections for Bi at 287 and 370 MeV, Proc. Radiochim. Acta 1, 135-139(2011).
12. Ninomiya, K., Omoto, T., Nakagaki, R., Takahashi, N., Shinohara, A., Sekimoto, S., Utsunomiya, T., Yashima, H., Shibata, S., Shima, T., Kinoshita, N., Matsumura, H., Hagiwara, M., Iwamoto, Y., Satoh, D., Caffee, M. W., Welten, K. C., Imamura, M., and Nishiizumi, K., Cross sections of ^{7}Be, ^{22}Na and ^{24}Na for geochemical and cosmochemical important elements by monoenergetic 287 and 370 MeV neutrons, Proc. Radiochim. Acta 1, 123-126(2011).
13. Niita, K., Matsuda N., Iwamoto, Y., Iwase, H., Sato, T., Nakashima, H., Sakamoto, Y. and Sihver, L. JAEA-Data/Code 2010-022 (2010).
14. Cugnon, J., Boudard, A., Leray, S. and Mancusi, D. J. Korean Phys. Soc., 59, 955-958 (2011).
15. Satoh, D., Sato, T., Shigyo, N. and Ishibashi, K. SCINFUL-QMD: Monte Carlo based computer code to calculate response function and detection efficiency of a liquid organic scintillator for neutron energies up to 3 GeV, JAEA-Data/Code, 2006-023 (2006)
16. Satoh, D., Sato, T., Endo, A., Yamaguchi, Y., Takada, M. and Ishibashi, K. Measurement of response functions of liquid organic scintillator for neutrons up to 800 MeV, J. Nucl. Sci. Technol., **43**, 714-719 (2006).
17. Iwamoto, Y., Hagiwara, M., Satoh, D., Iwase, H., Yashima, H., Itoga, T., Sato, T., Nakane, Y., Nakashima, H., Sakamoto, Y., Matsumoto, T., Masuda, A., Nishiyama, J., Tamii, A., Hatanaka, K., Theis, C., Feldbaumer, E., Jaegerhofer, L., Pioch, C., Mares, V. and Nakamura, T. Quasi-monoenergetic neutron energy spectra for 246 and 389 MeV $^{7}Li(p,n)$ reactions at angles from 0˚ to 30˚, Nucl. Instr. and Meth., A**629**, 43 -49(2011).
18. Firestone, R. B. and Shirley, V. S. Table of Isotopes, 8th edition , John Wiley and Sons, New York, (1996).
19. Nelson, W. R., Hirayama, H. and Rogers, D. W. O. The EGS4 code system, SLAC-265, Stanford Linear Accelerator Center, Stanford University (1985).
20. Michel, R., Gloris, M., Protoschill, J., Herpers, Ulrich, Kuhnhenn, J., Sudbrock, F., Malmborg, P. and Kubik, P. Cross sections for the production of radionuclides by proton-induced reactions on W, Ta, Pb and Bi from thresholds up to 2.6 GeV, J. Nucl. Sci and Technol., supplement **2**, 242 -245(2002).
21. Schiekel, Th., Sudbrock, F., Herpers, U., Gloris, M., Lange, H. -J., Leya, I., Michel, R., Dittrich-Hannen, B., Synal, H. -A., Suter, M., Kubik, P.W., Blann, M. and Filges, D. Nuclide production by proton-induced reactions on elements ($6 \leq Z \leq 29$) in the energy range from 200 MeV to 400 MeV, Nucl. Instr. and Meth., B**114**, 91 -119(1996).
22. Watanabe, Y., Fukahori, T., Kosako, K., Shigyo, N., Murata, T., Yamano, N., Hino, T., Maki, K., Nakashima, H., Odano, N. and Chiba, S. Proc. of Int. Conf. on Nuclear Data for Science and Technology, Santa Fe, USA, Sep.26-Oct.1,2004; AIP Conference Proc. 769, 326-331 (2005).
23. Watanabe, Y., Kosako, K., Kunieda, S., Chiba, S., Fujimoto, R., Harada, H., Kawai, M., Maekawa, F., Murata, T., Nakashima, H., Niita, K., Shigyo, N., Shimakawa, S.,

Yamano, N. and Fukahori, T. J. Korean Phys. Soc., 59, 1040-1045 (2011).

Table 1. The physical properties of radioactive nuclides.

target	product	half-life	Gamma-ray Energy[keV]	Branching ratio[%]
^{209}Bi	^{201}Bi	1.7h	629.1	26
^{209}Bi	^{202}Bi	1.72h	422.1	83.7
^{209}Bi	^{203}Bi	11.76h	820.2	29.6
^{209}Bi	^{204}Bi	11.22h	374.8	81.8
^{209}Bi	^{205}Bi	15.31d	703.5	31.1
^{209}Bi	^{206}Bi	6.243d	803.1	98.9
^{209}Bi	^{183g}Os	13h	381.8	89.6
^{209}Bi	^{200}Pb	21.5h	147.7	38.2
^{209}Bi	^{201}Pb	9.33h	331.2	76.9
^{59}Co	^{56}Co	77.27d	846.8	99.9
^{59}Co	^{57}Co	271.8d	122.1	85.6
^{59}Co	^{58}Co	70.82d	810.8	99.4
^{59}Co	^{52}Mn	5.591d	744.2	90.6
^{59}Co	^{54}Mn	312.3d	834.8	100

Table 2. Reaction cross section of nuclides induced by 386 MeV neutrons.

target	product	cross section[mb]		
^{209}Bi	^{201}Bi	38	±	13
^{209}Bi	^{202}Bi	54	±	18
^{209}Bi	^{203}Bi	63	±	18
^{209}Bi	^{204}Bi	57	±	18
^{209}Bi	^{205}Bi	76	±	26
^{209}Bi	^{206}Bi	71	±	25
^{209}Bi	^{183g}Os	7.4	±	2.4
^{209}Bi	^{200}Pb	74	±	21
^{209}Bi	^{201}Pb	100	±	28
^{59}Co	^{56}Co	8.0	±	2.5
^{59}Co	^{57}Co	36	±	11
^{59}Co	^{58}Co	65	±	21
^{59}Co	^{52}Mn	9.4	±	3.3
^{59}Co	^{54}Mn	44	±	12